PERGAMON

Journal of Structural Geology 22 (2000) 471–487

JOURNAL OF STRUCTURAL GEOLOGY

www.elsevier.nl/locate/jstrugeo

Processes controlling the shrinkage of porphyroclasts in gabbroic shear zones

Thomas Kenkmann

Institut für Mineralogie, Museum für Naturkunde, Zentralinstitut der Humboldt-Universität Berlin, Invalidenstraße 43, D-10115 Berlin, Germany

Received 5 May 1999; accepted 19 November 1999

Abstract

This paper presents microstructural and geochemical data on amphibole and clinopyroxene porphyroclasts collected in amphibolite-facies ultramylonites of the Ivrea–Verbano zone, Italy. The well-rounded porphyroclasts show a concentration of defects, including (100) twins, stacking faults, free dislocations, subgrains and microcracks within their rims that indicate stress concentrations. Localised deformation within the margins of porphyroclasts increases reaction kinetics and supports amphibole/clinopyroxene replacement reactions and heterogeneous plagioclase nucleation. In addition to microcracking and/or subgrain rotation these metamorphic reactions lead to a marginal grain-size reduction and the shrinkage of porphyroclasts. In order to correlate the defect concentration at the rim of porphyroclasts with stresses, a finite-element inclusion–matrix model is used. It depends on the degree of bonding between inclusion and matrix whether strong stress concentrations within the rim of the inclusion occur. For well-coupled two-phase systems, shear stresses within the rim of the inclusion can reach a magnitude many times the magnitude of the matrix stresses. Marginal stress concentrations do not evolve if inclusion and matrix are decoupled. This may indicate that mechanically decoupled porphyroclasts can survive to very large strains.

1. Introduction

Mylonitic shear zones are believed to contribute significantly to deformation in the middle and lower crust (e.g. Brodie and Rutter, 1987). They may even control the rheology of large parts of the continental lithosphere. Mylonites usually contain porphyroclasts, which occur in a wide range of sizes and shapes, and which represent relicts of the undeformed host rock. They are relatively rigid inclusions embedded in a fine-grained, ductile matrix. Porphyroclasts often consist of a weakly- to undeformed core and a deformed fine-grained mantle, elongated with two wings stretching away from the core (Passchier and Sokoutis, 1993). Many studies focus on porphyroclasts as kinematic indicators (e.g. Passchier and Simpson, 1986). For example, winged porphyroclasts with δ- or σ-geometry are well known as important shear-sense indicators. Moreover, porphyroclasts and their surroundings allow insights into flow properties of mylonite zones. They affect the rheology and the mechanical behaviour of a mylonite and may locally cause inhomogeneous plastic flow. The presence of relatively rigid inclusions in a weaker matrix commonly increases the strength of an aggregate. The effect of debonding and interface slip of inclusion–matrix systems on the mechanical response of materials has been evaluated in fibre ceramic–matrix and metal–matrix composites (e.g. Meyer et al., 1993). Recently, the role of incoherent interfaces has also been investigated for porphyroclast–matrix systems of mylonites with respect to strain and stress effects (Ildefonse and Mancktelow, 1993; Odonne, 1994; Kenkmann and Dresen, 1998). Sliding along the interface and opening of tensile voids in the pressure shadows may lead to a pressure sensitivity and a transient mechanical response of mylonites that enhances strain localisation. Slip may occur either by diffusion-accommodated grain boundary sliding or as a brittle

E-mail address: thomas.kenkmann@rz.hu-berlin.de (T. Kenkmann).

0191-8141/00/$ - see front matter
PII: S0191-8141(99)00177-7

stick-slip mechanism accompanied by crack–seal mechanisms in the pressure shadows.

So far, little attention has been paid to the porphyroclasts themselves. Nevertheless, they play a crucial role in understanding mylonitisation processes because the mechanisms of grain size reduction in ductile shear zones can be studied in situ along the rim of porphyroclasts. The deformation and shrinkage of porphyroclasts is intimately linked to the formation of a mylonitic matrix since porphyroclasts serve as suppliers for new matrix grains. The results of this study indicate that local stress concentrations, which occur within the rim of porphyroclasts, are required to initiate an effective grain size reduction in ductile shear zones. The first part of this paper presents microstructural and geochemical data on amphibole and clinopyroxene porphyroclasts collected in amphibolite-facies ultramylonites of the Ivrea–Verbano Zone, Italy. In the second part a numerical model, which is discussed in detail by Kenkmann and Dresen (1998), is used to determine the stress distribution within porphyroclasts. Stresses are calculated for coherent and incoherent interfaces between porphyroclast and matrix. In the discussion of this paper, an attempt is made to link the microstructural and geochemical data qualitatively with the stress distribution and to infer mechanisms responsible for the shrinkage of porphyroclasts.

2. Geological and petrological setting

The samples are obtained from an ultramylonite shear zone of the Ivrea–Verbano Zone, Italy (Fig. 1). The Ivrea–Verbano Zone is part of the pre-Alpidic basement of the southern Alps and is considered to represent a section through a segment of thinned lower to middle continental crust (Zingg, 1983; Rutter et al., 1993). The base of the section is formed by gabbros, ultramafic bodies, and diorites intruding into a sequence of metapelites and metabasites (Rivalenti et al., 1981; Handy and Zingg, 1991; Schmid, 1993; Henk et al., 1997). The metamorphic grade decreases steadily from granulite-facies near the Insubric Line (NW) to amphibolite-facies near the Pogallo Line (SE). Magmatic underplating and regional metamorphism of the Ivrea–Verbano Zone occurred in the late Palaeozoic (300–285 Ma). The intrusion of basic magmas was coeval with the onset of crustal extension and the

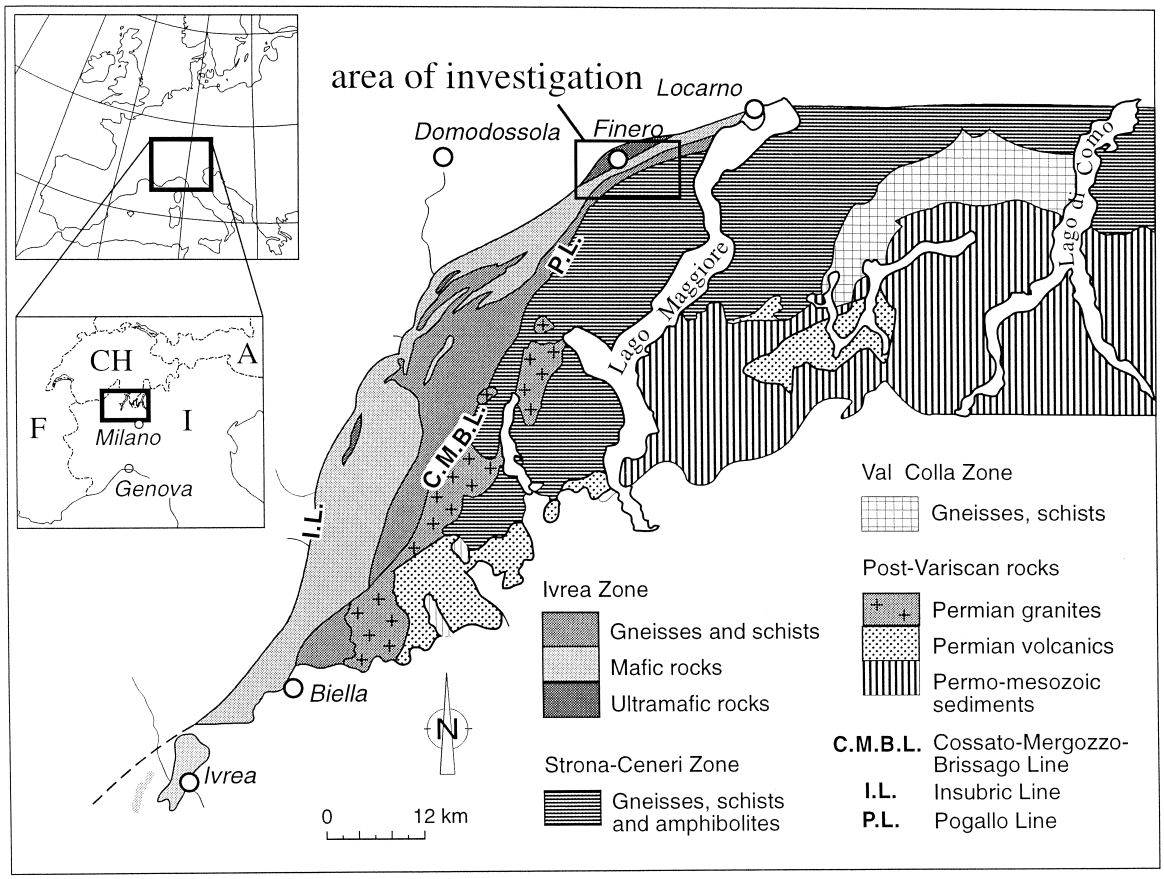

Fig. 1. Map of the Ivrea–Verbano Zone and the adjacent Strona Ceneri Zone, northern Italy. The square focuses the area of investigation.

formation of high temperature shear zones (Rutter et al., 1993). The high temperature shear zones comprised a braided network of low angle extensional faults (Brodie and Rutter, 1987; Handy, 1987) which are inferred to have controlled the rheology of the attenuating crust in the Late Palaeozoic and Early Mesozoic (Brodie et al., 1989). Localised mylonitic shearing under granulite and retrograde amphibolite-facies conditions affected the mafic body as well as the meta-sedimentary cover rocks. Final uplift, tilting and exposure of the deep crustal sequence resulted from polyphase Alpine transpressional tectonics (Handy and Zingg, 1991).

The investigated shear zone is located in a metagabbro close to hornblende–peridotites of the Finero Complex (Fig. 1). Locally, the shear zone marks the transition between mafic and ultramafic units. The samples were collected in the riverbed of the *Toce Cannobina*, about 1 km southeast of Finero. Plagioclase, hornblende, clinopyroxene, garnet, and ilmenite are the major minerals within the shear zone rocks and the predeformational metagabbro assemblage. The metagabbro displays a weak magmatic foliation and stretching lineation formed by subhedral amphiboles and clinopyroxenes. Adjacent to the shear zone the gabbro displays *C′*-type shear bands (Berthé et al., 1979), which form with dominantly recrystallised plagioclase. The shear bands wrap around stiffer lenses of amphibole, clinopyroxene, and garnet. Macroscopic structures of the shear zone consist of a well-developed foliation, lineation and banding from mm to m scale. The width of the exposed shear zone is about 8 m. The ultramylonites themselves consist of a mixed polyphase matrix (amphibole/clinopyroxene–plagioclase–ilmenite assemblage) with a grain size of 10–50 μm, which contains up to 5% porphyroclasts. A kinematic analysis of the shear zone reveals non-coaxial flow with an estimated dextral displacement of > 0.3 km (Kenkmann, 1997).

The granulite-facies host rock assemblage has been re-equilibrated at a temperature of 650–700°C and a pressure of maximum 7.5 kbar (Franz, personal communication) prior to the formation of the ultramylonites. The shear zone was active under retrograde conditions ranging from 650 to 500°C (6–4 kbar) as derived by the amphibole thermobarometer of Laird and Albee (1981) and the plagioclase–hornblende-thermometer of Spear (1980). Amphibolitisation of clinopyroxene is common in the fine-grained mylonites, but in some layers clinopyroxene still occurs frequently in the polyphase mylonitic matrix. This compositional banding defines the foliation of the mylonites. A static growth of epidote, actinolite, Mg-chlorite, sphene and albite is observed in parts of the shear zone. This greenschist-facies alteration paragenesis is restricted to narrow zones.

This study focuses on porphyroclasts embedded into the polyphase ultramylonitic matrix. The investigated porphyroclasts are either amphiboles (pargasite to ferropargasite, after nomenclature of Leake, 1997) or clinopyroxenes (diopside or augite). The composition of amphibole in the matrix is dominantly edenitic and plagioclase composition varies from Ab_{50} to Ab_{75}. The presence of fluids during deformation is inferred from inter and intragranular fluid inclusions and an increasing amphibole/clinopyroxene ratio in the shear zone rocks.

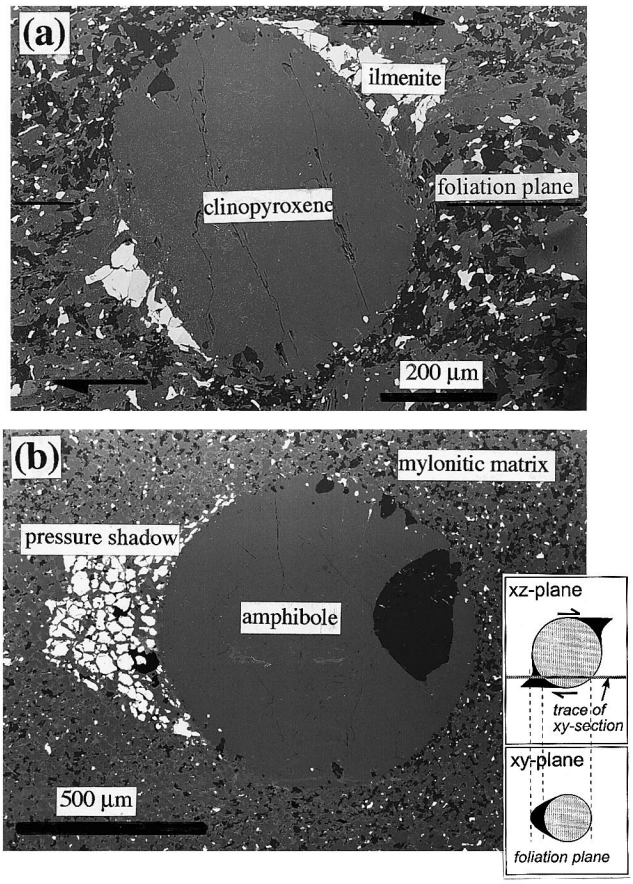

Fig. 2. SEM-BSE images of a clinopyroxene (a) and an amphibole porphyroclast (b). (a) Section normal to the foliation plane and parallel to the stretching lineation (*xz*-plane), arrows indicate the sense of shear. (b) Section parallel to the foliation plane (*xy*-plane). The section cuts the porphyroclast eccentrically in such a way that one of the pressure shadows (upper or lower) is visible. Porphyroclasts are well rounded and have ellipsoidal or circular shapes. They are embedded in a fine-grained mylonitic matrix consisting dominantly of amphibole (grey), plagioclase (dark) and ilmenite (light). All porphyroclasts are associated with ilmenite aggregates, which grow in the pressure shadows.

3. Analytical techniques

Thin sections were prepared from the shear zone rocks. They were cut in the *xz*-plane of the strain ellip-

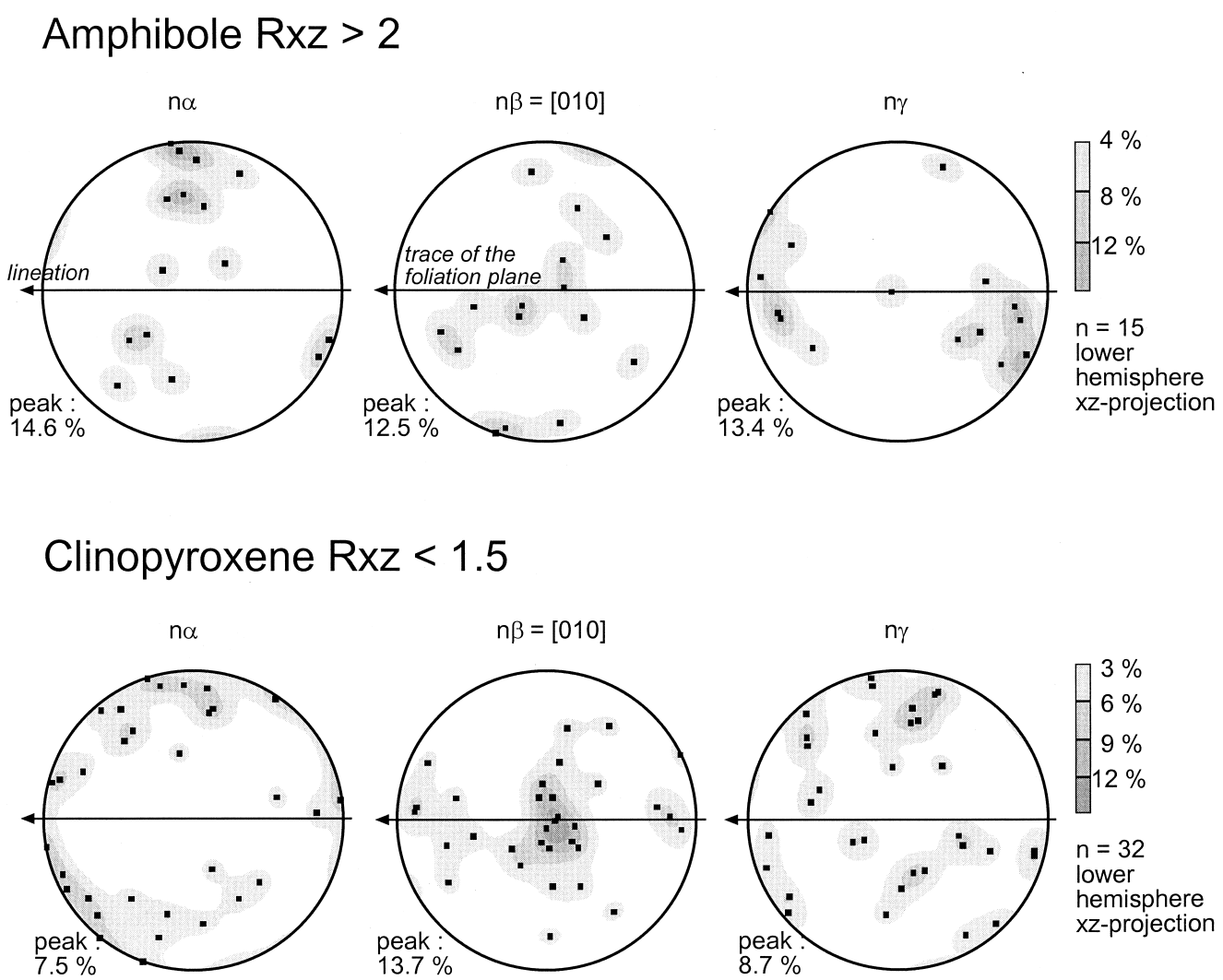

Fig. 3. Pole figures show the orientations of optical axes for amphibole and clinopyroxene porphyroclasts with $R_{xz} > 2$ and $R_{xz} < 1.5$, respectively. Projections were made in the *xz*-plane, that is, they are normal to the rock foliation and parallel to stretching lineation. Dots represent single measurements. Counting area: 6.7% (amphibole) and 3.1% (clinopyroxene) of the hemisphere. Contour levels give the number of measurements in percentage per 1% of the hemisphere (Robin and Jowett, 1986). A discussion of the distribution pattern is given in the text.

soid (parallel to lineation and normal to foliation) and in the *xy*-plane (parallel to foliation). Fabrics and microstructures were studied using optical microscopy and a scanning electron microscope (SEM ZEISS-DSM 962) in backscattered-electron mode. Quantitative chemical point analyses of amphibole, clinopyroxene and plagioclase were carried out with wavelength-dispersive spectrometers (WDX) on a CAMECA SX 100 microprobe at 15 kV acceleration voltage and a beam current of 20 nA using doubly-polished thin sections. The counting time was 10–30 s depending on the element. The analytical error is ~1% rel. for the major elements and ~5% rel. for minor elements. The detection limits under the specified working conditions vary between 0.05 and 0.1 wt.%. Element mapping of Mg and Al was performed on a CAMECA SX 50 microprobe at 20 kV and 20 nA in a systematic sweep such that the entire surface of a porphyroclast was analysed.

The charge-balance method described by Robinson et al. (1982) was used to calculate the stoichiometry of amphiboles. The total number of cations is 13, excluding Ca, Na and K. All cations were recalculated to 23 oxygens. For transmission electron microscopy (TEM), selected samples were ion-thinned using a GATAN ion mill. A PHILIPS CM 200 TWIN microscope operating at 200 kV and equipped with an EDX system was used to study microstructures within porphyroclasts. Dislocation densities were measured counting dislocation endpoints from plates with magnifications between 20 000 and 50 000 (Underwood, 1970, p. 157, eq. 6.10).

4. Microstructural observations and geochemical studies

4.1. Shape and orientation of porphyroclasts

The porphyroclasts of the investigated ultramylonites are well-rounded σ-clasts and their diameters range from 400 to 2000 μm (Fig. 2). Amphibole and clinopyroxene porphyroclasts can be divided into two groups with regard to their shapes: spherical porphyroclasts (aspect ratio $R_{xz} < 1.5$) (Fig. 2a, b) and ellipsoidal porphyroclasts (aspect ratio $R_{xz} > 2$). Ellipsoidal amphibole porphyroclasts are weakly prolate and have a ratio $R_{xy}/R_{yz} \sim 1.1$, whereas clinopyroxene porphyroclasts have oblate shapes with $R_{xy}/R_{yz} \sim 0.85$. The long axis of ellipsoidal amphibole porphyroclasts is commonly oriented with 10–30° oblique to the shear plane. The shape-preferred orientation of ellipsoidal amphibole porphyroclasts with $R_{xz} > 2$ correlate with an optically preferred orientation (Fig. 3). The optical axis $n\alpha$ shows a maximum normal to the foliation, $n\gamma$ has a maximum in an acute angle to the rock lineation and $n\beta = [010]$ has a girdle-like distribution normal to rock lineation. Although the texture is not fully determined by optical axes alone, it appears that the *c*-axes are preferentially oriented in an acute angle to the rock lineation since $n\gamma$ and [001] deviate by 30° on average. For flow types with vorticity numbers $0 < W_k < 1$, there is a critical aspect ratio, R_c, below which inclusions rotate permanently and above which they cease to rotate at positions of either stable or unstable equilibrium (Hanmer and Passchier, 1991). The shape and optical orientation of ellipsoidal amphibole porphyroclasts suggest that they exceed R_c and have reached a stable position during non-coaxial flow.

In contrast, circular clinopyroxene porphyroclasts with $R_{xz} < 1.5$ show $n\beta = [010]$ clustering in the shear plane normal to the rock lineation (Fig. 3). The optical axis $n\alpha$ forms a *xz*-girdle and $n\gamma$ shows an irregular distribution pattern. It is inferred from this pattern that circular clinopyroxene porphyroclasts have rotated during non-coaxial deformation. The rotation axis may coincide with [010].

Most of the porphyroclasts in the shear zone represent forward-rotated σ-type porphyroclasts (Passchier and Simpson, 1986) (Fig. 2b). However, the steep inclination of the long axis of the porphyroclast in Fig. 2(a) with respect to the foliation together with the tail 'step-up' to the right indicates that also backward-rotated σ-type porphyroclasts occur within the shear zone. This means, that an additional pure-shear component is superimposed to the simple shear deformation (Simpson and De Paor, 1993). Rolling during non-coaxial flow may lead to the formation of circular shapes by marginal erosion, which is discussed in detail in the following sections. The relevance of mechanical anisotropies of amphibole and clinopyroxene seems to be subordinate to the effect of rolling.

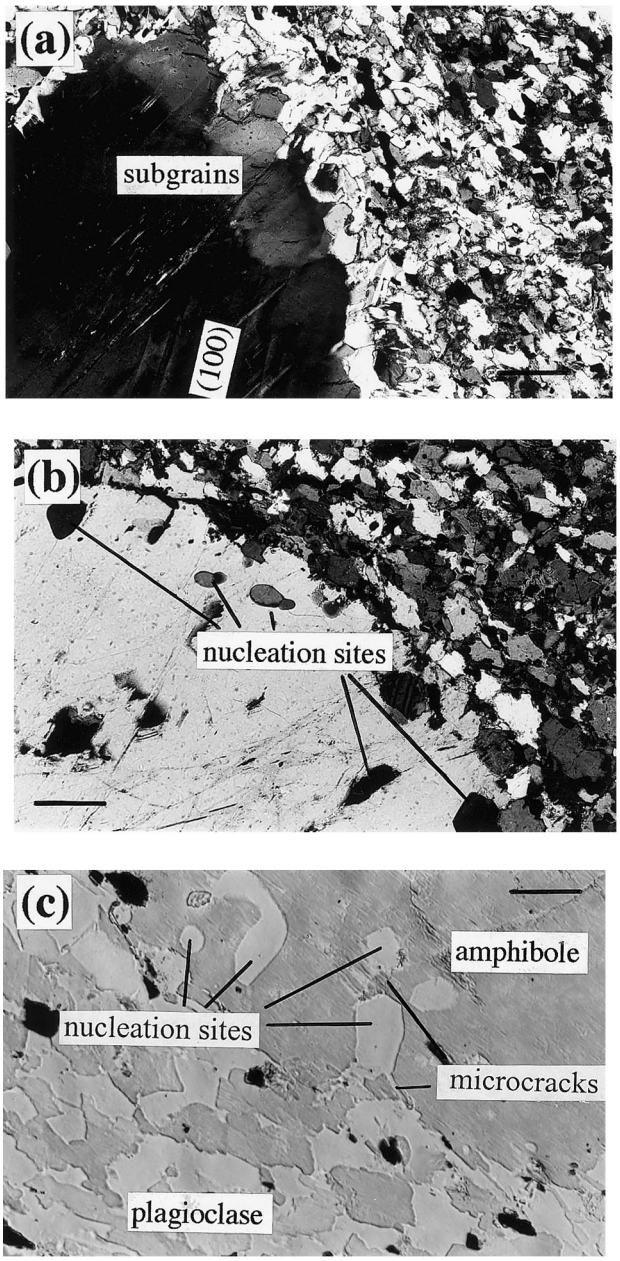

Fig. 4. Photomicrographs of amphibole porphyroclasts and surrounding mylonitic matrix (*xy*-sections). (a) Subgrains form within the rim of the porphyroclast, {110} cracks and (100) twins within the porphyroclast can be seen in the lower left (crossed polars, scale bar: 85 μm). (b) Plagioclase inclusions occur frequently within the rim of the porphyroclast. Their phase boundaries are convex-outward and indicate growing on the expense of amphibole (crossed polars, scale bar: 35 μm). (c) Due to heterogeneous plagioclase nucleation, the interface of porphyroclast and matrix strongly bulges into the porphyroclast. Exposed marginal remnants of the porphyroclast separate along microcracks from the porphyroclast and are dragged into the mylonitic matrix (oblique polars, oblique illumination, scale bar: 15 μm).

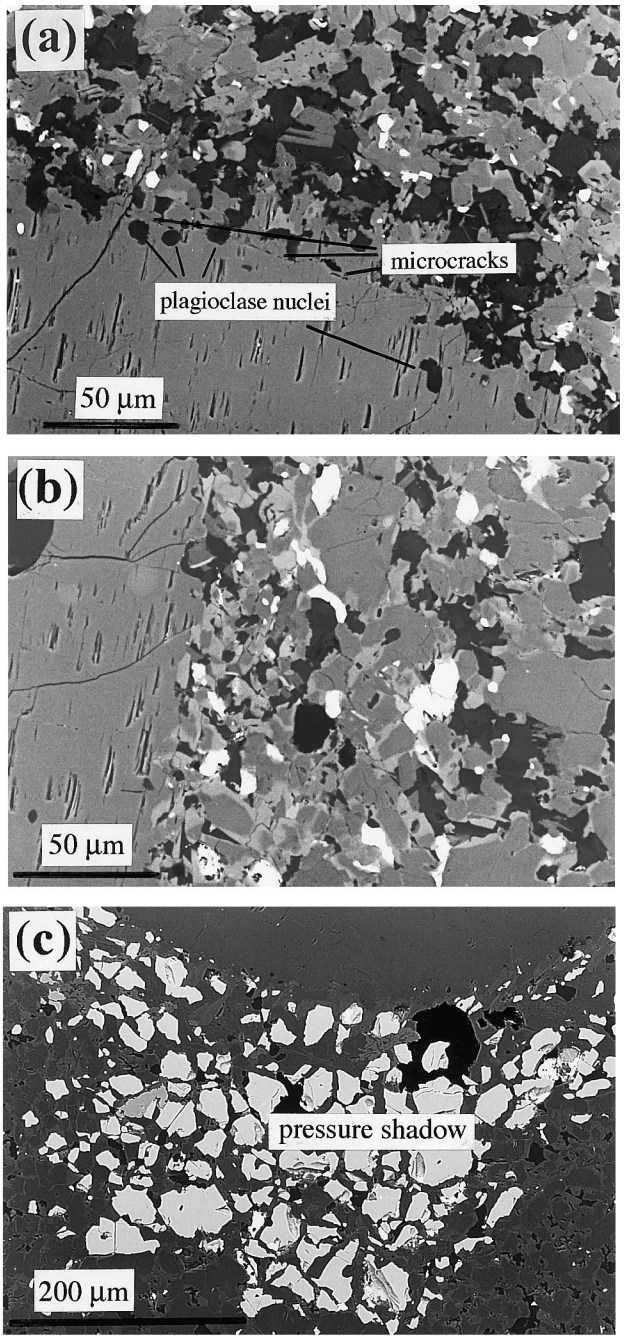

Fig. 5. SEM-BSE images showing three different interface segments of an amphibole porphyroclast cut in the *xy*-plane (parallel to the foliation). See also Fig. 2(b). The frequency of plagioclase nucleation within the rim of the porphyroclast systematically varies along its surface. Adjacent to pressure shadows (c) plagioclase nucleation does not occur. On the opposite side of the porphyroclast (a) plagioclase neomineralisation is clearly visible within the porphyroclast, (b) shows the side of the porphyroclast facing to the *y*-direction. The interface of porphyroclast and matrix consists of ragged edges. Amphibole grains that lose contact with the porphyroclast will be incorporated into the ultramylonitic matrix to form new mylonitic grains of 10–50 μm. Mechanisms of grain separation are {110} microfracturing and subgrain rotation.

4.2. Microstructure

Most of the hornblende and clinopyroxene porphyroclasts display well-developed, σ-type pressure shadows filled with ilmenite. Recrystallised mantles and tails consisting of recrystallised porphyroclast material, commonly observed around quartz or feldspar porphyroclasts of granitic mylonites, are absent in the investigated rocks.

Although the porphyroclasts are well rounded (Fig. 2) it is important to notice that the interfaces of porphyroclast and matrix are not smooth on the scale of the matrix grain size. Figs. 4 and 5 show that the surface of porphyroclasts consists of ragged edges and partly frays out because plagioclase nucleates at various sites within the margin of the porphyroclasts (Figs. 4c and 5a). At several sites, the interface of porphyroclast and matrix bulges into the porphyroclast. The concentration of plagioclase inclusions within the rim of the porphyroclasts even leads to a poikilitic microstructure (Fig. 4c), predominantly at those parts facing the fine-grained mylonitic matrix. Small plagioclase nuclei have nearly circular shapes to minimise the required surface energy. Larger nuclei commonly grow along rational crystallographic directions of amphibole and clinopyroxene, dominantly along {110} and (100) cleavage planes, respectively.

Optical micrographs show that the interior of amphibole porphyroclasts contains some mechanical twins along (100) (Fig. 4a). A patchy extinction within the marginal area of the porphyroclasts points to the formation of subgrains (Fig. 4a) or a lattice distortion induced by microcracking. On the basis of TEM analysis some free dislocations are found. Simple dislocation walls consist of arrays of parallel dislocations. It remains ambiguous whether they have formed during high-temperature subgrain rotation processes or during crack healing. Additionally, microcracks occur parallel to {110} and increase in abundance towards the interface (Fig. 5a).

Clinopyroxene porphyroclasts, comprising undulatory extinction and bending of exsolution lamellae in optical micrographs, show that they are internally strained. The distortion is concentrated within the marginal area of the porphyroclasts. Bright field electron micrographs (Fig. 6) show that a range of planar defects and a variety of dislocation substructures exist within the rim of clinopyroxene porphyroclasts. They are displayed by isolated curved dislocations, isolated straight dislocations, stacking faults (Fig. 6a) as well as simple and complex dislocation networks (Fig. 6b). The dislocation walls form boundaries of subgrains that are internally dislocation-free (Fig. 6c). The geometry of the subgrain boundaries varies from simple tiltwalls (Fig. 6c) to more complex dislocation networks. The latter

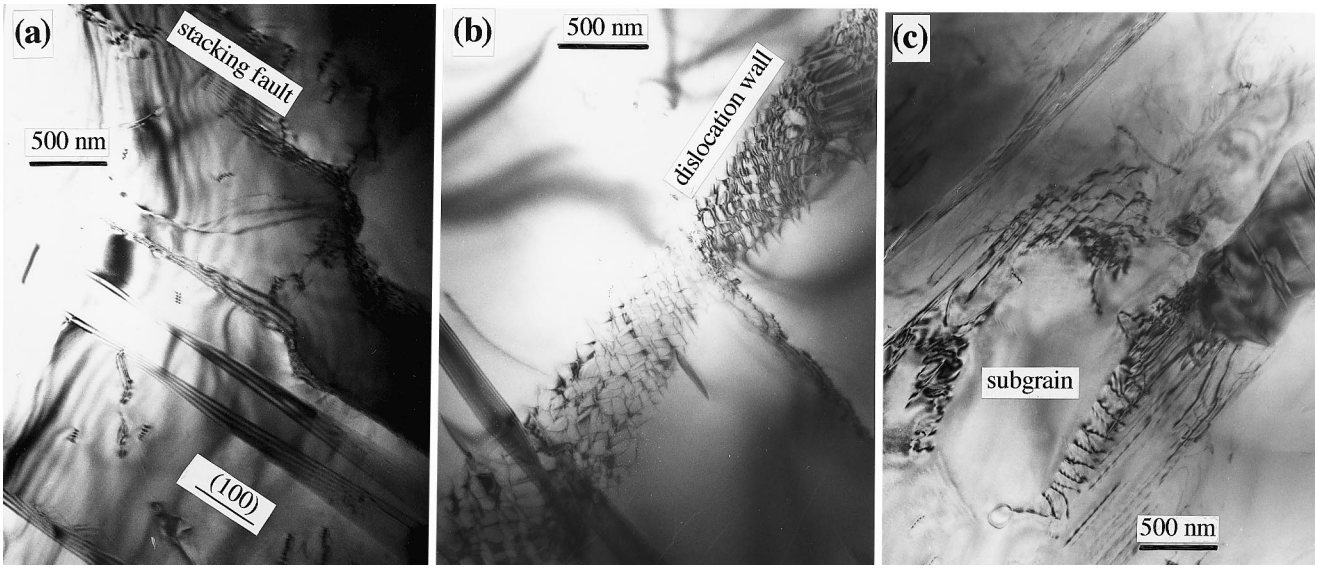

Fig. 6. TEM images (bright field) of clinopyroxene porphyroclasts. (a) Free dislocations, (100) stacking faults and (100) twin lamellae, found near the interface of porphyroclast and matrix. The stacking faults are formed when partial dislocations move apart. (b) Complex dislocation wall indicates climb and cross slip of dislocations at high-temperature conditions. Stacking faults intersect the dislocation network at the lower left. (c) This clinopyroxene subgrain is bound by parallel arrays of dislocations and is internally strain-free. Dislocations are dominantly straight. Generally, subgrains are more abundant near the porphyroclast rim than in the centre of porphyroclast. (d) (100) lamellae are preferential sites used for crack propagation near the rim of porphyroclasts. Geochemical alteration products like amphiboles and sheet silicates occur along these planes. (e) Irregularly running dislocation walls and trails of fluid inclusions indicate healed cracks. (f) Fluid inclusions string along a dislocation wall (out of contrast). Their shape is determined by (100) and (001) directions. (g) High resolution TEM image of a coherent grain boundary parallel (101) between clinopyroxene and amphibole formed at immediate vicinity to the porphyroclasts surface.

indicate climb and cross slip of dislocations at high temperature conditions (Fig. 6b). Subgrains range in size between 0.3 and 2.5 μm. These microstructures indicate that dislocations are relatively free to climb. Mechanical twinning is observed along (100) planes (Fig. 6d).

The interior of the porphyroclasts is poor in free dislocations but some dislocation walls occur. Most of the described defects concentrate near the rim of the porphyroclasts. The density of free dislocations increases from $5.1 \times 10^8\,cm^{-2}$ in the centre of porphyroclasts to $4.4 \times 10^9\,cm^{-2}$ at the interface of porphyroclast and matrix. Dislocation densities were measured at different parts along the rim, but the number of measurements (28) is insufficient to derive iso-dislocation density contours. In addition to that, a strong contribution to deformation near the porphyroclast rim stems from microcracks forming along the (100) and (001) anisotropies of exsolution lamellae and twin planes (Fig. 6d). Dislocations associated with these cracks develop in response to crack propagation. Unlike dislocations formed at high temperature conditions, these dislocations always have straight traces and do not form regular networks (Fig. 6e). Dislocation walls formed by crack healing run irregularly and are always associated with trails of fluid inclusion (Fig. 6e and f). Such healed cracks are widely present in the outer zone of porphyroclasts (Fig. 6e and f).

Due to the growth of plagioclase within the rim of porphyroclasts, the interface porphyroclast–matrix consists of ragged edges. Marginal parts become partly separated in such a way that only bridges of amphibole and clinopyroxene remain which maintain contact to the porphyroclast. These exposed parts of the porphyroclasts are fairly breakable. Shear forces that are induced by the flow of the mylonitic matrix cause the separation of the exposed parts along microfractures. The isolated grains rotate and are dragged into the mylonitic matrix. If clinopyroxene or amphibole lose contact with the porphyroclast they stem from, they will be incorporated into the ultramylonitic matrix to form new mylonitic grains of 10–50 μm. Two distinct processes are responsible for the mechanical separation of grains from the porphyroclasts: Amphibole predominantly shows subgrain rotation (Fig. 4a) and cracking along {110} (Figs. 4c and 5a), clinopyroxene displays microcracking along (100) and (001) (Fig. 6d–f) and progressive subgrain rotation (Fig. 6b and c).

4.3. Geochemical zonations

The results of quantitative microprobe analyses (Figs. 7 and 8; Tables 1 and 2) reveal the existence of

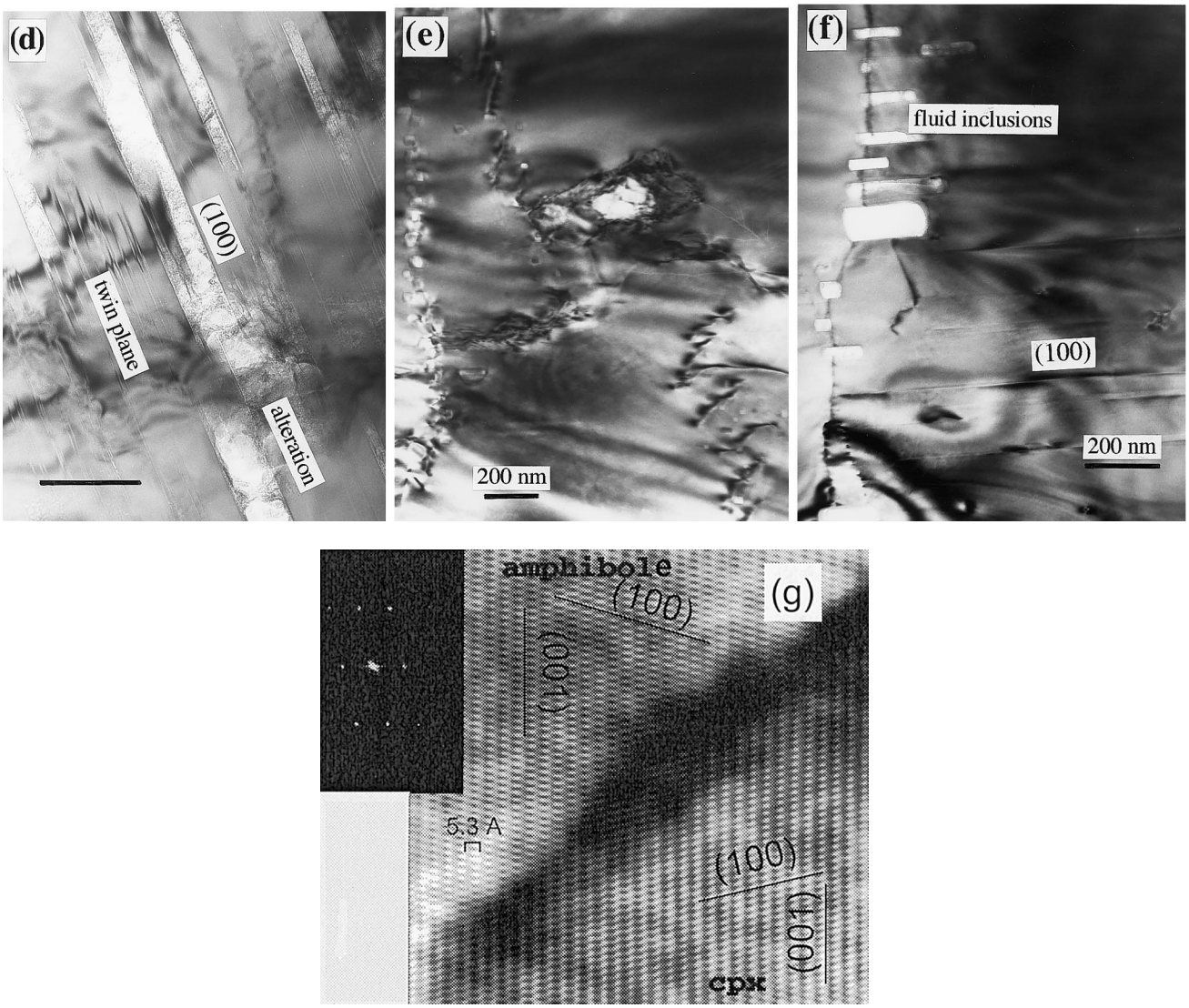

Fig. 6 (*continued*)

geochemical zonations in both amphibole and clinopyroxene porphyroclasts. Amphibole porphyroclasts (pargasite to ferropargasite) show a loss in Al, Ti, (Na) and an enrichment of Si and Mg near the interface. Systematic differences in composition also occur between the rim of amphibole porphyroclasts and surrounded amphibole grains of the mylonitic matrix (Table 1). The latter are edenitic in composition, that is they are again depleted in Al, Ti and Na and enriched in Si and Mg with respect to the porphyroclast rim. Thus, the chemical composition of the rim is intermediate between that of the matrix grains and the centre of the clast.

Reactions at the edge of amphibole porphyroclasts lead to compositional changes in amphibole and the nucleation of plagioclase and may be approximated as follows (see also Table 2):

$$1\mathrm{AMP1} + 0.28\mathrm{PLA1} + 0.7\mathrm{SiO_2} \rightarrow 0.83\mathrm{AMP2} + 0.11\mathrm{AMP3} + 0.56\mathrm{PLA2} + 0.17\mathrm{FeO} + 0.05\mathrm{H_2O} \quad (1)$$

Input data for the balanced reaction are provided by microprobe analyses from an amphibole porphyroclast (core and rim), together with analyses of amphibole and plagioclase grains occurring at the rim of the porphyroclast. In order to decrease the number of components to seven (SiO_2, Al_2O_3, FeO, MgO, CaO, Na_2O, H_2O) in the balanced reaction all Fe^{3+} is recalculated to Fe^{2+}. The trend in amphibole composition from the centre of the porphyroclasts towards the matrix grains can be explained with coupled edenite, Ti-tschermakite and Al-tschermakite substitutions (Laird and Albee, 1981; Kenkmann, 1997) and is consistent with the inferred retrograde metamorphic

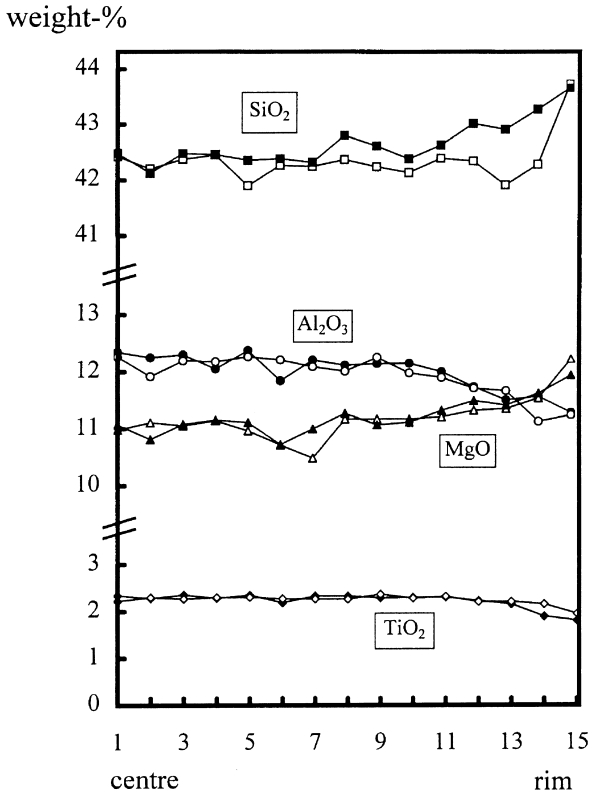

Fig. 7. Two microprobe profiles across an amphibole porphyroclast. Each of them consists of 15 measurement points. The profile starts in the centre (point 1) and reaches the rim (point 15) of the porphyroclast. Profiles are oriented parallel to reference axes of the mylonites: the profile with open symbols is oriented normal to the foliation. Black symbols represent an orientation parallel to foliation and lineation. In both profiles, SiO_2 and MgO are enriched, whereas Al_2O_3 and TiO_2 are depleted towards the interface of porphyroclast and matrix.

evolution in the shear zone. Coupled substitution reactions involve the growth of plagioclase, which is consistent with the observed concentration of plagioclase nuclei within the porphyroclast's rim. The heterogeneous nucleation of plagioclase within the rim of amphibole porphyroclasts due to chemical disequilibrium initiates a phase mixtures of hornblende and plagioclase, which remains a charactistic feature for the entire mylonitic matrix (Kenkmann, 1997).

Zonations in amphibole porphyroclasts indicate diffusion processes. In contrast to matrix grains, the porphyroclasts retain their original composition within their centre due to their much larger grain sizes. This implies that matrix grains have recrystallised without compositional difference and change their composition through diffusion after recrystallisation, maybe during subsequent cooling. However, the differences in composition between matrix grains and the rim of porphyroclasts show that additional compositional changes must have occurred during formation of the matrix grains. New grains with a different composition can either be formed by heterogeneous nucleation or by chemically-induced grain boundary migration without nucleation (Cumbest et al., 1989).

In clinopyroxene porphyroclasts Al, Fe and Ti are depleted towards the rim with respect to average concentration in the porphyroclast centre. There is a minor increase of Ca and Mg near the interface of porphyroclast and matrix. The zonations affect the entire rim of the porphyroclasts (Fig. 8). Like in amphibole, the differences in composition reflect the compositional adjustment to decreasing metamorphic grade. Chemical alteration of clinopyroxene and the replacement reaction of clinopyroxene by amphibole may be quantified as follows (see also Table 2):

$$1\mathrm{CPX1} + 0.02\mathrm{PLA1} + 0.09\mathrm{H_2O} \rightarrow 0.61\mathrm{CPX2} + 0.09\mathrm{AMP2} + 0.1\mathrm{PLA2} + 0.14\mathrm{SiO_2} + 0.13\mathrm{CaO} \quad (2)$$

The replacement reaction of pyroxene by amphibole is driven by the infiltration of water and takes place by nucleation and growth of amphibole lamellae (Veblen and Buseck, 1981) mostly parallel to cleavage planes and microcracks (Fig. 6d). The orientation of amphibole and pyroxene chains remains unchanged, which is suggested by the investigation of the electron-diffraction patterns of neighbouring clinopyroxene and amphibole crystals. Fig. 6(g) shows such a coherent boundary parallel (101) between clinopyroxene and amphibole at immediate vicinity to the porphyroclasts surface. The (100) of amphibole and clinopyroxene is rotated by 30°. However, new amphibole grains formed also by a heterogeneous nucleation mechanism along the interface of porphyroclast and matrix. This is suggested in cases when no crystallographic relationship is observed between the new and host grains. The balanced reaction also indicates the growth of quartz. Quartz was sometimes found as very small grains (1 μm) along the interface of porphyroclast and matrix. However, the amount of quartz seems to be overestimated in the proposed reaction.

5. Numerical modelling of the stress distribution within porphyroclasts

It is suggested, that the driving force for the concentration of deformation microstructures combined with the various mineralogical changes and reactions within the rim of porphyroclasts are local variations in stress. To investigate the role of stress concentrations in porphyroclasts, a finite element model (commercial code MARC Analysis Research Corporation 1994) was designed. The stress distribution is calculated in an inclusion embedded in a softer matrix with both materials deforming in power law creep. A detailed

description of the applied numerical model was previously given by Kenkmann and Dresen (1998), where stresses of a matrix surrounding a porphyroclast were presented. Accordingly, below, only a brief review of the model design is given.

Flow of inclusion and matrix material is modelled using a creep equation of the general form $\dot{e} = A_{(700^\circ C)}\sigma^n$, where $\dot{e}$ is the axial strain rate, A is the pre-exponential factor at an assumed temperature of 700°C, σ is the differential stress, and n is the stress exponent. Matrix and inclusion are modelled with parameters derived for diabase (Caristan, 1982) and wet clinopyroxenite (Boland and Tullis, 1986), respectively. Axial strain is converted to plane strain using a factor of $0.5 \times 3^{((n+1)/2)}$, following the model of Chester (1995). The model is deformed in simple shear at constant shear stress of 25 MPa. The stress distribution within the inclusion is investigated for various degrees of coupling of the inclusion and the matrix. This is possible, because inclusion and matrix elements do not share common nodes. Thus, elements from the matrix and the inclusion can shift with respect to each other. Two types of decoupling can be modelled along the interface: sliding and opening of gaps. The amount of slip along the interface of inclusion and matrix can be modified using an algorithm for cohesive shear friction for the interface (Kenkmann and Dresen, 1998). The opening of gaps occurs along the interface if a given traction normal to the interface is exceeded. These gaps may represent pressure shadows of natural porphyroclasts.

The stress distribution within the porphyroclast is summarised in Fig. 9. The stress magnitude depends on the coupling behaviour of matrix and inclusion. Peak differential stresses are concentrated along the rim of the porphyroclast for a fully coupled interface (Fig. 9a). If clast and matrix are strongly coupled stress may increase along the interface of porphyroclast and matrix locally to a factor of 20–30 with respect to the average matrix stress (Fig. 9a and c). Interface sliding reverses the stress pattern within the inclusion because slip along the interface relaxes marginal distortion (Fig. 9b and d) and stresses are not completely transmitted into the inclusion. If gaps are allowed to open (pressure shadows) and matrix and inclusion are only partially coupled, the magnitude of differential stress is high at the interface and relatively low near the gaps (Fig. 9c and d).

6. Discussion

6.1. Comparison between deformation microstructures and the numerical model

Deformation microstructures in clinopyroxene porphyroclasts demonstrate changes in the mode of deformation. Microstructures partly indicate deformation at high temperatures (and/or low strain rates). In particular subgrain formation typical for recovery-controlled dislocation creep, is characteristic for deformation at high temperatures. Unlike this, microstructures like (100) twins and glide planes with kinks, straight dislocations and microcracks indicate deformation at low

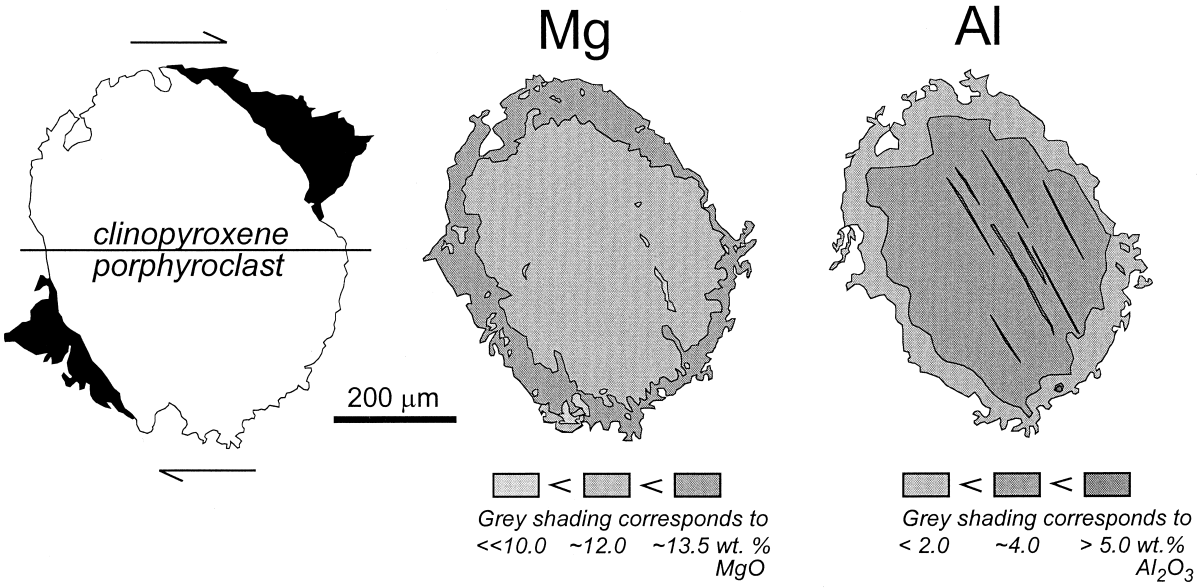

Fig. 8. Mg and Al distribution within a clinopyroxene porphyroclast (see also Fig. 2a) based on automatic microprobe mapping. Contours were equilibrated quantitatively, using single point analyses. Changes in Mg and Al are clearly visible towards the rim of the porphyroclast. Mg increases and Al is depleted at the margin. The affected zone has a width of 20–100 μm and is developed along the entire rim.

Table 1
Representative mineral chemistry of amphibole and clinopyroxene porphyroclasts and plagioclase (wt.%)

Plagioclase		SiO_2	Al_2O_3	CaO	MnO	FeO	BaO	Na_2O	K_2O	wt.%	Ab	An	Or
K30-51	unrecryst.	56.72	27.72	9.78	0.00	0.32	0.05	6.02	0.06	100.69	52.5	47.1	0.4
K30-52	unrecryst.	57.15	27.40	9.50	0.00	0.38	0.00	6.16	0.08	100.67	53.7	45.8	0.5
K47-38	unrecryst.	56.16	27.41	10.07	0.00	0.12	0.01	5.93	0.06	100.46	51.4	48.3	0.3
K30-71	recryst./neom.	59.15	25.68	7.45	0.03	0.50	0.03	7.29	0.05	100.18	63.7	36.0	0.3
K30-81	recryst./neom.	58.69	25.71	7.51	0.00	0.32	0.00	7.35	0.05	99.63	63.7	36.0	0.3
K47-42	recryst./neom.	57.12	26.45	8.64	0.02	0.17	0.00	6.75	0.04	99.20	58.4	41.3	0.2
K47-51	recryst./neom.	56.88	26.54	9.05	0.05	0.12	0.07	6.69	0.04	99.46	57.1	42.7	0.2
Clinopyroxene		SiO_2	TiO_2	Al_2O_3	Fe_2O_3	Cr_2O_3	MgO	CaO	MnO	FeO	Na_2O	K_2O	wt.%
K30-615	clast	50.25	0.46	4.43	2.45	0.02	12.16	20.89	0.38	7.96	0.80	0.00	99.80
K30-815	clast	50.15	0.44	4.30	2.48	0.05	12.08	20.79	0.37	8.12	0.80	0.00	99.58
K30-915	clast	50.39	0.47	4.09	2.16	0.00	11.84	20.92	0.43	8.54	0.82	0.00	99.65
K30-461	clast-rim	52.32	0.19	1.79	1.33	0.04	13.53	21.94	0.37	8.01	0.46	0.00	99.96
K30-916	clast-rim	52.40	0.19	1.69	1.74	0.00	13.49	22.30	0.43	7.65	0.46	0.00	100.33
K30-615	clast-rim	53.05	0.12	1.53	0.58	0.04	13.51	22.29	0.36	8.18	0.51	0.00	100.17
Amphibole		SiO_2	TiO_2	$A1_2O_3$	Fe_2O_3	Cr_2O_3	MgO	CaO	MnO	FeO	Na_2O	K_2O	wt.%
K47-23	clast	42.65	2.23	11.89	3.06	0.08	11.61	11.51	0.25	11.43	2.44	0.48	97.55
K47-11	clast	41.56	2.27	12.61	6.09	0.04	11.21	11.28	0.28	10.08	2.31	0.71	98.43
K47-24	clast-rim	43.08	2.30	11.92	1.96	0.07	11.60	11.77	0.14	12.36	2.34	0.50	98.03
K30-118	clast-rim	43.43	2.16	11.76	1.07	0.04	11.48	11.96	0.22	13.07	2.01	0.79	97.95
K47-39	matrix	44.53	1.84	10.80	2.73	0.08	12.88	11.88	0.11	10.39	2.01	0.40	97.57
K30-36	matrix	44.90	1.76	10.22	2.93	0.00	12.57	11.77	0.16	11.03	1.67	0.89	97.90
K30-119	matrix	44.33	1.73	10.84	2.78	0.02	12.60	11.91	0.22	10.69	1.83	0.65	97.58

temperature (and/or high strain rates). According to the retrogressive metamorphic evolution in the shear zone, climb and recovery in clinopyroxene play an important part during the early deformation history at upper amphibolite-facies conditions. At steadily decreasing metamorphic grade accompanying the uplift of the rocks, these processes are followed by dislocation glide, twinning and finally microcracking.

Both amphibole and clinopyroxene are believed to represent minerals of high shear strength resistance (Hacker and Christie, 1990; Skrotzki, 1994) because dynamic recovery by climb and cross slip is often hindered by dislocation dissociation. Furthermore, exsolution in clinopyroxene leads to effects of precipitation hardening (Skrotzki, 1994). The critical resolved shear stress required for mechanical twinning in clinopyroxene is about 140 MPa (Kollé and Blacic, 1982). The shear strength of amphibole and clinopyroxene is expected to be higher than the bulk shear strength of strongly localised shear zones that may probably range between 50 and 100 MPa (Ord and Christie, 1984). The occurrence of mechanical twins in clinopyroxene and amphibole porphyroclasts indicates that shear stresses in the order of 140 MPa were reached locally, specifically within the margin of porphyroclasts. The concentration of deformation microstructures like free dislocations and microcracks within the margin of porphyroclasts also support the observation that stresses increase towards the rim of porphyroclasts. Although no precise gradient in defect concentration from the porphyroclast centre to the interface is available, defects within the porphyroclasts seem to increase abruptly over a short distance from the porphyroclast–matrix interface. The apparent deficiency of free dislocations, microcracks and twins within the centre of porphyroclasts suggests that only those relict grains survive to large strains and form porphyroclasts in ductile shear zones, which were initially undeformed and remain undeformed during non-coaxial flow. In those porphyroclasts, most of the imposed strain is converted into rotation (spin). Plastic strain may then be dominantly restricted to the rim of porphyroclasts. From the optical orientation pattern (Fig. 3) of circular clinopyroxene porphyroclasts it is concluded that clinopyroxene grains preferentially build up porphyroclasts, whose [010] axis was initially oriented in the foliation plane and normal to the stretching lineation.

The concentration of defects and stress at the rim of porphyroclasts is in agreement with the results of the numerical model and suggests that the investigated porphyroclasts are mechanically well coupled to the matrix. However, since the distribution of dislocation densities is not fully determined in the entire porphyroclast, comparisons with the stress distribution based on

Table 2
Mineral chemistry of amphibole, clinopyroxene and plagioclase used for the balanced reactions (1) and (2) in the text

	CPX1 clast-centre	CPX2 clast-rim	AMP1 clast-centre	AMP2 clast-rim	AMP3 matrix	PLA1 unrecryst.	PLA2 recryst.
SiO_2	49.90	52.21	41.97	43.38	44.62	56.71	58.77
TiO_2	0.50	0.15	2.34	2.16	1.71	–	–
Al_2O_3	4.33	1.42	12.35	10.85	10.00	26.45	25.32
Cr_2O_3	0.03	0.04	0.01	0.05	0.05	–	–
Fe_2O_3	2.92	1.66	4.02	2.83	1.41	–	–
MgO	12.26	13.65	11.20	11.81	11.68	0.00	0.00
CaO	20.66	22.34	11.49	11.64	11.96	10.16	7.33
MnO	0.38	0.38	0.23	0.17	0.07	0.04	0.02
FeO	7.45	7.15	11.39	11.78	13.20	0.07	0.13
Na_2O	0.85	0.45	2.40	1.80	1.43	6.15	7.34
K_2O	0.00	0.00	0.52	1.04	0.96	0.03	0.05
wt.%	99.28	99.45	97.91	97.49	97.09	99.61	98.96
	6 cations		23 cations			8 cations	
Si	1.879	1.975	6.219	6.441	6.644	2.56	2.65
Ti	0.014	0.004	0.261	0.241	0.192	–	–
Al	0.192	0.063	2.156	1.899	1.755	1.41	1.35
Cr	0.001	0.001	0.001	0.005	0.006	–	–
Fe^{3+}	0.083	0.047	0.448	0.316	0.158	–	–
Mg	0.688	0.762	2.475	2.614	2.593	0.00	0.00
Ca	0.833	0.897	1.823	1.851	1.908	0.49	0.35
Mn	0.012	0.012	0.029	0.021	0.008	0.00	0.00
Fe^{2+}	0.235	0.224	1.411	1.463	1.644	0.00	0.01
Na	0.062	0.033	0.690	0.517	0.411	0.54	0.64
K	0.000	0.000	0.098	0.196	0.182	0.00	0.00
at.%	4.000	4.000	15.611	15.564	15.501	5.00	5.00

the FE-modelling remain difficult. Using the available data it is suggested that the model in Fig. 9(a) (completely coupled interface) and Fig. 9(c) (partly coupled interface: no sliding, but opening of gaps) are the best descriptions of the natural conditions. If decoupling occurs, it seems to be restricted to those parts that are affected by tensile forces normal to the interface. These areas are the pressure shadows where ilmenite successively precipitates.

6.2. Effects of the stress distribution on metamorphic reactions and grain size

As mentioned before, nucleation and growth processes contribute to the shrinkage and marginal erosion of porphyroclasts. The frequency and size of plagioclase nuclei within the rim of porphyroclasts changes as a function of their position. Adjacent to pressure shadows, plagioclase nucleation is of minor

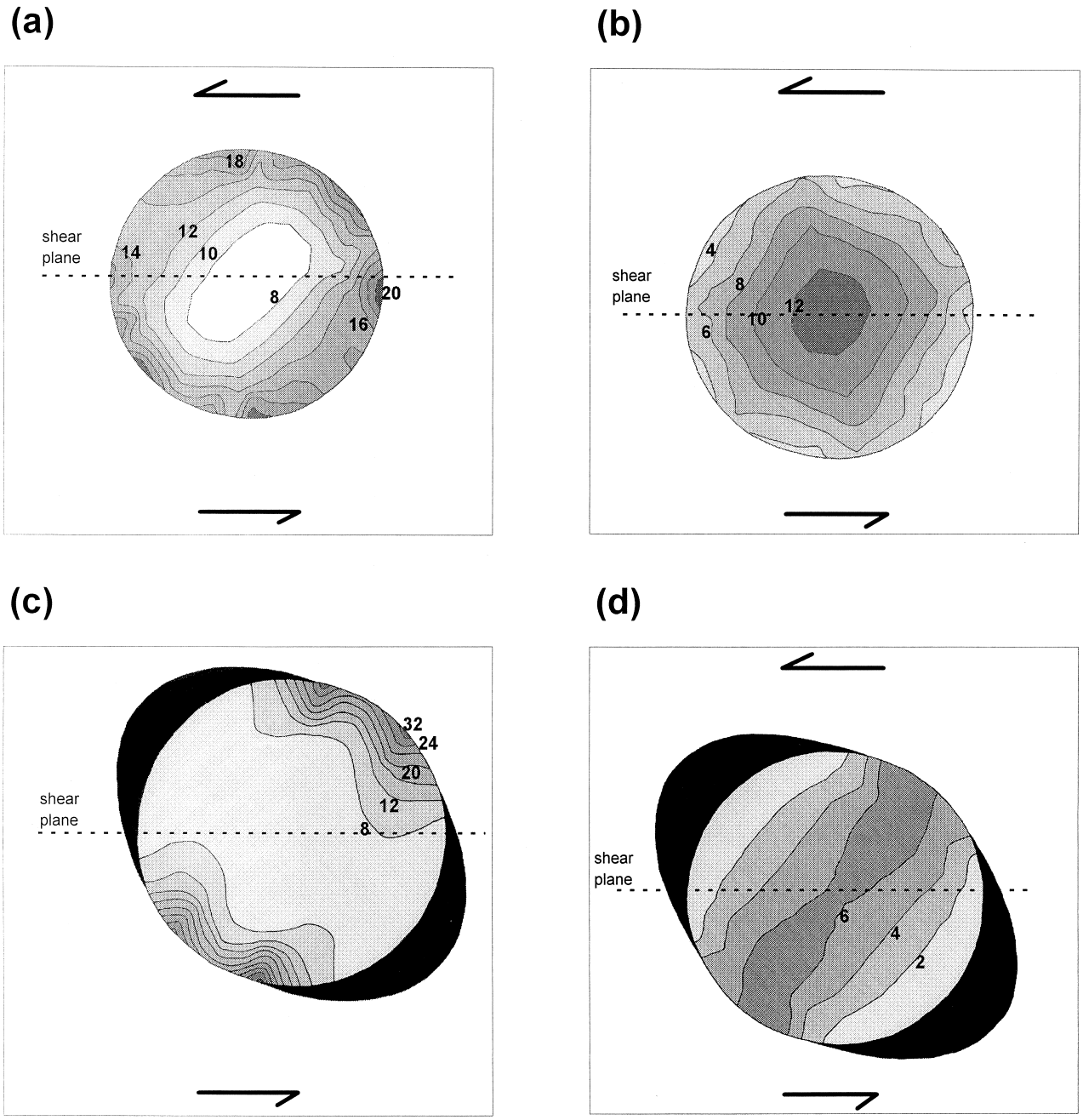

Fig. 9. Differential stress distributions within a spherical inclusion embedded in a weaker matrix obtained with the numerical model under different bonding conditions. Differential stress is normalised to the stress of the mylonitic matrix. The shear strain is 0.45 ± 0.03. (a) No gap opening, no interface sliding. (b) No gap opening, interface sliding. (c) Gap opening, no interface sliding. (d) Gap opening, interface sliding.

importance (Fig. 5c). Here, ilmenite is precipitated in low stress domains of the surrounding matrix and this indicates that solution-precipitation creep and/or diffusion creep play an important role in the deformation of the mylonites. On the opposite side of the porphyroclast (facing the fine-grained matrix) nucleation of plagioclase occurs more frequently (Fig. 5a). This distribution may be explained in terms of stress gradients produced by the porphyroclast in the surrounding mylonitic matrix (Kenkmann and Dresen, 1998). Similar observations were made by Simpson and Wintsch (1989), who found a strong positive correlation between predicted high normal stress sites and the occurrence of myrmekites along the surface of porphyroclasts. They concluded that the addition of extra strain energy along the high-stress sides of the porphyroclasts might have localised the reaction at these sites.

Stable stress gradients along and normal to the surface of porphyroclasts affect the chemical potential of individual chemical components (Gresens, 1966). Under anisotropic stress the chemical potential at the surface of a grain (e.g. porphyroclast) is given by $\mu = F + \sigma_n V$, where F is the specific Helmholtz free energy and V is the specific volume of the mineral phase, μ the chemical potential of the migrating component at the grain surface, and σ_n is the component of stress normal to the surface. Because a porphyroclast is under anisotropic stress during deformation, all surface segments of different orientations have different normal stress values. Thus, there are differences in chemical potential from segment to segment, inducing diffusion along the porphyroclasts surface (Raj, 1982; Wheeler, 1992). Pressure gradients are capable of increasing the concentration of some components at certain sites. They therefore also increase the possibility for the nucleation of new phases at these sites in which the enriched components are major constituents. If a reaction involves a net volume decrease, it is favoured at sites of high normal stress (Simpson and Wintsch, 1989). This study shows that the preferential formation of ilmenite and amphibole grains in or near the pressure shadows indicates a migration of Fe, Mg and Ti to the lower normal stress regions. Likewise, the preferential nucleation of plagioclase in higher normal stress regions suggests a migration of Na to high-stress parts. As previously shown, nucleation and growth of one species also involves the replacement of another species. The replacement reaction must lower the Gibbs free energy of the whole system.

However, nucleation is not a function of concentration alone, but it also depends on kinetic effects like the diffusion rate of individual components and the activation energy for nucleation, which in turn depend on the stored strain energy. In the highly strained rim of the porphyroclasts suitable sites for heterogeneous nucleation of plagioclase exist on linear or planar defects which are energetically more favourable than in an unstrained structure. However, the free energies from chemical disequilibrium are expected to be at least as high as the deformational energies (Kruse and Stünitz, 1999).

The study has shown that heterogeneous nucleation of plagioclase within the margin of both amphibole and clinopyroxene porphyroclasts causes the formation of new mylonitic grains and leads to the decay and shrinkage of the porphyroclasts. This process also causes the phase mixtures of hornblende and plagioclase grains that characterise the entire mylonitic matrix of the investigated mafic shear zone. To maintain this phase mixture in the mylonitic matrix steadily, a preferential heterogeneous nucleation of hornblende at plagioclase grain boundaries, and vice versa, is required (Kenkmann, 1997; Kruse and Stünitz, 1999; Newman et al., 1999).

Thermally activated diffusion in defect-free clinopyroxene is extremely slow under the conditions of deformation; this is particularly valid for multi-component diffusion (Brady, 1993). However, zonations in clinopyroxene porphyroclasts reach widths of up to 150 μm. This can be explained in terms of a deformation-enhanced and fluid-assisted diffusion. Plastic deformation that occurred in the rim of porphyroclasts increases diffusion coefficients through the pipe effect. At lower temperature conditions microcracks significantly increase the permeability of the porphyroclasts. Microcracks also enhance reaction kinetics by increasing the grain surface area available for reaction.

It is conspicuous that there is positive correlation between predicted high normal stress sites (Fig. 9c) and domains of enhanced plagioclase nucleation within the rim of porphyroclasts (Figs. 2a, b and 5), whereas the geochemical zoning pattern of the porphyroclasts does not show a correlation to these regions, but occurs all round the rim of the porphyroclasts (Fig. 8). This distribution seems to correlate to a stress pattern presented in Fig. 9(a). There are three ways to explain these apparent discrepancies: (a) the zonation of the porphyroclasts has occurred after deformation during subsequent cooling (this is discussed in Section 4.3), (b) a correlation between stresses and the geochemical zonation does not occur, or, (c) the geochemical zonation of porphyroclasts points to rotation processes of the porphyroclasts. Porphyroclasts with a low aspect ratio rotate forward or backwards, as pointed out in Section 4.1. Thus, during rotation any part of the porphyroclast's surface runs through the high stress sites as well as through the low stress sites. Deformation microstructures and geochemical alteration gained in the high stress regions are rotated towards the low stress domains. Thus, a concentration of deformation microstructures and geochemical alteration occurs

within the complete rim of the porphyroclast. Since plagioclase nucleation sites are not frequently found in the low-stress sites, the porphyroclast must have effectively shrunk during rotation in such a way that the detachable parts containing a large number of plagioclase nuclei are dragged into the mylonitic matrix (Fig. 4).

From the preceding statements the following conclusions can be drawn: The occurrence of marginal stress concentrations along the rims of porphyroclasts induces diffusional mass transfers and enhances plastic and brittle deformation, which in turn enhances reaction kinetics in various ways. The geochemical and mechanical processes may work simultaneously and lead to marginal erosion and shrinkage of porphyroclasts and the origin of fine-grained mylonites. To produce fine grains of clinopyroxene and amphibole, stress concentrations may be required. However, a paleopiezometric link between stresses occurring within the margin of porphyroclasts and the grain size, which evolves at the edge of the porphyroclasts, cannot be used because dynamic recrystallisation processes in the sense of Urai et al. (1986) and Drury and Urai (1990) do not occur. The final grain size in the matrix depends on several processes including (a) the subgrain size within the rim of porphyroclasts (at high temperature conditions), (b) the fracture density within the rim of porphyroclasts (at lower temperatures) and (c) the relative rates of nucleation and growth of plagioclase and amphibole. Process (c) affects the final grain size because of different pressure and temperature sensitivities of the nucleation rate and growth rate. The effect of different temperatures on the nucleation and growth rate (Joanny et al., 1991; Riedel and Karato, 1997) has to be taken into account since a long deformation history has left traces in the mylonites. It is generally valid that the grain size is small when nucleation dominates over growth, and vice versa (Riedel and Karato, 1997). Furthermore, kinetic barriers for nucleation as discussed before may evolve in different ways along the surface of the porphyroclasts.

It is generally assumed that deformation in mylonites is a steady state process that is maintained by a balance between work hardening (increase in dislocation density) and work softening effects (decrease in dislocation density by recovery) (Means, 1981). However, for the onset of mylonitisation special circumstances seem to be required: To start the grain size reduction in amphibole and clinopyroxene bearing rocks local stress concentrations, which enhance the defect density on one side and intensify diffusional mass flux and reaction kinetics on the other side, are of crucial importance. A precursor stage to complete and pervasive mylonitisation is C'-type shear bands in the metagabbro at the investigated locality (see Section 2), in which plagioclase recrystallises dynamically. These shear bands wrap around stiffer lenses of amphibole and clinopyroxene. It is inferred that at the edges of such lenses the required stress concentrations are induced to start the grain size reduction in amphibole and clinopyroxene. Once the shear zone has established and localised, the surface of porphyroclasts, representing relicts of these lenses, can be designated as the active mylonitisation front of mylonitic shear zones.

If porphyroclast and matrix are decoupled, differential stresses in the porphyroclast are distinctly lower than for a coupled interface. Presumably, the clasts will then survive to larger strains. The flow stress concentrates in the centre of the porphyroclast and therefore recrystallisation and/or microfracturing within the rim should be much less developed.

7. Conclusions

The following conclusions can be drawn regarding processes controlling the shrinkage of porphyroclasts:

1. The concentration of deformation microstructures like subgrains, free dislocations, microcracks and twins within the margin of porphyroclasts suggests that stresses increase within porphyroclasts towards the porphyroclast–matrix interface. Stress concentrations are likely to enhance diffusional mass transfer and enhance reaction kinetics in various ways along the rims of porphyroclasts.
2. The 'in situ' grain size reduction along the surface of porphyroclasts is the result of a combined mechanical–geochemical process: Stress-induced subgrain rotation recrystallisation and microfracturing on one side and clinopyroxene/amphibole replacement reactions and heterogeneous plagioclase nucleation on the other side lead to marginal erosion and the shrinkage of porphyroclasts.
3. Numerical modelling suggests that local stress concentrations occur at the interface of porphyroclast and matrix if mechanical bonding between both of them is strong. Marginal stress concentrations accelerate shrinking of porphyroclasts in various ways. They may even be necessary prerequisites to produce fine-grained amphibole and clinopyroxene aggregates. If decoupling of porphyroclast and matrix occurs, porphyroclasts may survive to very large strains.

Acknowledgements

This research was supported by the GeoForschungs-Zentrum Potsdam and Museum für Naturkunde, Humboldt-Universität Berlin. The paper has benefitted from discussions with G. Dresen and R. Porth. I

thank Martyn Drury and two anonymous reviewers for helpful comments and constructive criticisms.

References

Berthé, D., Choukroune, P., Jegouzo, P., 1979. Orthogneiss, mylonite and non-coaxial deformation of granites: the example of the south Amorican shear zone. Journal of Structural Geology 1, 31–41.

Boland, J.N., Tullis, T.E., 1986. Deformation behavior of wet and dry clinopyroxenite in the brittle to ductile transition region. American Geophysical Union Geophysical Monograph 36, 35–50.

Brady, J.B., 1993. Diffusion data for silicate minerals, glasses, and liquids. In: Ahrens, T.H. (Ed.), AGU Handbook of Physical Constants.

Brodie, K.H., Rutter, E.H., 1987. Deep crustal extensional faulting in the Ivrea Zone of Northern Italy. Tectonophysics 140, 193–212.

Brodie, K.H., Rex, D., Rutter, E.H., 1989. On the age of deep crustal extensional faulting in the Ivrea zone, northern Italy. In: Coward, M.P., Diedrich, D., Park, R.G. (Eds.), Alpine tectonics, Geological Society of London Special Publication 45, pp. 203–210.

Caristan, Y., 1982. The transition from high-temperature creep to fracture in Maryland diabase. Journal of Geophysical Research 87, 6781–6790.

Chester, F.M., 1995. A rheologic model for wet crust applied to strike-slip faults. Journal of Geophysical Research 100, 13033–13044.

Cumbest, R.J., Drury, M.R., van Roermund, H.L.M., Simpson, C., 1989. Dynamic recrystallization and chemical evolution of clinoamphibole from Senja, Norway. Contributions to Mineralogy and Petrology 101, 339–349.

Drury, M., Urai, J.L., 1990. Deformation-related recrystallization processes. Tectonophysics 172, 235–253.

Gresens, R.L., 1966. The effect of structurally produced pressure gradients on diffusion in rocks. Journal of Geology 74, 307–321.

Hacker, B.R., Christie, J.M., 1990. Brittle/ductile and plastic/cataclastic transitions in experimentally deformed and metamorphosed amphibolite. American Geophysical Union. Geophysical Monograph 56, 127–147.

Handy, M.R., 1987. The structure, age and kinematics of the Pogallo fault zone; southern Alps, northwestern Italy. Eclogae Geologicae Helvetiae 80, 593–632.

Handy, M.R., Zingg, A., 1991. The tectonic and rheological evolution of an attenuated cross section of the continental crust. Ivrea crustal section, southern Alps, northwestern Italy and southern Switzerland. Geological Society of America Bulletin 103, 236–253.

Hanmer, S., Passchier, C., 1991. Shear-sense indicators. A review. Geological Survey of Canada, 90-17, 70 pp.

Henk, A., Franz, L., Teufel, S., Oncken, O., 1997. Magmatic underplating, extension and crustal reequilibration: Insights from a cross-section through the Ivrea Zone and Strona–Ceneri Zone, Northern Italy. Journal of Geology 105, 367–377.

Ildefonse, B., Mancktelow, N.S., 1993. Deformation around rigid particles: the influence of slip at the particle/matrix interface. Tectonophysics 221, 345–359.

Joanny, V., van Roermund, H., Lardeaux, J.M., 1991. The clinopyroxene/plagioclase symplectite in retrograde eclogites: a potential geothermobarometer. Geologische Rundschau 80, 303–320.

Kenkmann, T., 1997. Verformungslokalisation in gabbroiden Gesteinen—Mikrostrukturelle und mineralogische Untersuchungen in einer Hochtemperatur-Scherzone der Ivrea-Zone, Italien. Ph.D thesis. Freie Universität Berlin, Scientific Technical Report 97, 141 pp., Potsdam.

Kenkmann, T., Dresen, G., 1998. Stress gradients around porphyroclasts: palaeopiezometric estimates and numerical modelling. Journal of Structural Geology 20, 163–173.

Kollé, J.J., Blacic, J.D., 1982. Deformation of single-crystal clinopyroxenes. 1. Mechanical twinning in diopside and hedenbergite. Journal of Geophysical Research 87, 4019–4034.

Kruse, R., Stünitz, H., 1999. Deformation mechanisms and phase distribution in mafic high-temperature mylonites from the Jotun Nappe, southern Norway. Tectonophysics 303, 223–249.

Laird, J., Albee, A.L., 1981. Pressure, temperature and time indicators in mafic schists. Their application to reconstructing the polymetamorphic history of Vermont. American Journal of Science 281, 127–175.

Leake, B.E., 1997. Nomenclature of amphiboles; report of the subcommittee on amphiboles in the International Mineralogical Association Commission on new minerals and mineral names. European Journal of Mineralogy 3, 623–651.

Means, W.D., 1981. The concept of steady-state foliation. Tectonophysics 78, 179–199.

Meyer, D.W., Cooper, R.F., Plesha, M.E., 1993. High-temperature creep and the interfacial mechanical response of a ceramic matrix composite. Acta Metallurgica et Materialia 41, 3157–3170.

Newman, J., Lamb, W.M., Drury, M.R., Vissers, R.L.M., 1999. Deformation processes in a peridotite shear zone: reaction softening by an H_2O-deficient, continuous net transfer reaction. Tectonophysics 303, 193–222.

Ord, A., Christie, J.M., 1984. Flow stresses from microstructures in mylonitic quarzites of the Moine Thrust zone, Assynt area, Scotland. Journal of Structural Geology 6, 639–654.

Passchier, C.W., Simpson, C., 1986. Porphyroclast systems as kinematic indicators. Journal of Structural Geology 8, 831–844.

Passchier, C.W., Sokoutis, D., 1993. Experimental modelling of mantled porphyroclasts. Journal of Structural Geology 15, 895–909.

Raj, R., 1982. Creep in polycrystalline aggregates by matter transport through a liquid phase. Journal of Geophysical Research 87, 4731–4739.

Riedel, M.R., Karato, S., 1997. Grain-size evolution in subducted oceanic lithosphere associated with the olivine-spinel transformation and its effects on rheology. Earth and Planetary Science Letters 148, 27–43.

Rivalenti, G., Garuti, G., Rossi, A., Siena, F., Sinigoi, S., 1981. Existence of different peridotite types and of a layered igneous complex in the Ivrea zone of the western Alps. Journal of Petrology 22, 127–153.

Robin, P.Y.F., Jowett, E.C., 1986. Computerized density contouration and statistical evaluation of orientation data using counting circles and continuous weighting functions. Tectonophysics 121, 207–233.

Robinson, P., Spear, F.S., Schumacher, J.C., Laird, J., Klein, C., Evans, B.W., Doolan, B.L., 1982. Phase relations of metamorphic amphiboles: natural occurrence and theory. In: Veblen, D.R., Ribbe, P.H. (Eds.), Amphiboles and other hydrous pyriboles-mineralogy. Reviews in Mineralogy 9B 227 pp.

Rutter, E.H., Brodie, K.H., Evans, P., 1993. Structural geometry, lower crustal magmatic underplating and lithospheric stretching in the Ivrea zone, Northern Italy. Journal of Structural Geology 15, 647–662.

Schmid, S.M., 1993. Ivrea Zone and adjacent southern alpine basement. In: Von Raumer, J.F., Neubauer, F. (Eds.), Pre mesozoic geology in the Alps, pp. 567–583.

Simpson, C., De Paor, D.G., 1993. Strain and kinematic analysis in general shear zones. Journal of Structural Geology 15, 1–20.

Simpson, C., Wintsch, R.P., 1989. Evidence for deformation-induced

K-feldspar replacement by myrmekite. Journal of Metamorphic Geology 7, 261–275.

Skrotzki, W., 1994. Defect structure and deformation mechanisms in naturally deformed augite and enstatite. Tectonophysics 229, 43–68.

Spear, F.S., 1980. NaSi = CaAl exchange equilibrium between plagioclase and amphibole. Contributions to Mineralogy and Petrology 72, 33–41.

Underwood, E.E., 1970. Quantitative stereology. Addison–Wesley, Reading, Massachusetts.

Urai, J.L., Means, W.D., Lister, G.S., 1986. Dynamic recrystallization of minerals. American Geophysical Union Geophysical Monograph 36, 161–199.

Veblen, D.R., Buseck, P.R., 1981. Hydrous pyriboles and sheet silicates in pyroxenes and uralites. Intergrowth microstructures and reaction mechanisms. American Mineralogist 66, 1107–1134.

Wheeler, J., 1992. Importance of pressure solution and Coble creep in the deformation of polymineralic rocks. Journal of Geophysical Research 97, 4579–4586.

Zingg, A., 1983. The Ivrea and Strona–Ceneri zones (Southern Alps, Ticino and N-Italy)—A review. Schweizerische Mineralogische und Petrographische Mitteilungen 63, 361–392.